https://dx.doi.org/10.1016/j.conbuildmat.2017.10.031

Resilience and Life-Cycle Performance of Smart Bridges with Shape Memory Alloy (SMA) -Cable-Based Bearings

Yue Zheng[1], You Dong[2*], and Yaohan Li[3]

Abstract:

Due to its unique properties within hazard mitigation, shape memory alloy (SMA) has been developed and adopted within the design and retrofit of civil infrastructures to improve the seismic performance. The performance benefit associated with the SMA bridges in a long term has not been well recognized by the decision maker, thus, the wide application of SMA within the civil infrastructures is still limited. This paper aims to apply the resilience and life-cycle loss assessment to the comparative performance assessment of novel and conventional bridges and to promote the application of novel materials within the civil engineering. Both the direct and indirect costs are considered within the life-cycle assessment process. Specifically, the corresponding structural performance, resilience, and life-cycle loss associated with different bridge systems are addressed. The methodology accounts for the life-cycle loss assessment considering the representative hazard scenarios that could happen within the investigated region. The proposed approach is applied to highway bridges with and without using the SMA-cable-based bearings. The benefit associated with the application of the proposed novel bearing is quantified in terms of resilience and life-cycle loss.

Keywords: Shape memory alloy; Earthquake; Fragility curve; Life-cycle loss; Comparative assessment; Resilience.

---

[1]Assistant Professor, Department of Bridge Engineering, Tongji University, Shanghai, China, yzheng@tongji.edu.cn

[2]Assistant Professor of Structural Engineering, Department of Civil and Environmental Engineering, The Hong Kong Polytechnic University, Hung Hom, Kowloon, Hong Kong, you.dong@polyu.edu.hk. *Corresponding Author.

[3]Department of Civil and Environmental Engineering, The Hong Kong Polytechnic University, Hung Hom, Kowloon, Hong Kong, yaohan.li@outlook.com

1. Introduction

Earthquakes can bring disastrous consequences to our society and economy. For instance, the 2015 Nepal earthquake killed nearly 9,000 people and more than 600,000 structures in Kathmandu and the nearby towns were either damaged or destroyed. Thus, it is of paramount importance to mitigate structural damage under seismic hazard. To address this concern, several seismic improvements have been adopted within the design codes to enhance seismic performance of bridges. Many studies showed that isolation devices can dissipate a large amount of energy as these devices introduce a discontinuity between the superstructure and substructure and reduce the energy transferred to the superstructure. Accordingly, isolation devices have been developed to reduce the bridge damage under seismic hazard and have been implemented with the structural design process, especial for the essential structures. The conventional isolation devices include lead-rubber bearings, high damping bearings, and magneto-rheological dampers, etc. (Ghobarah and Ali 1990; Warn and Whittaker 2004; Bhuiyan *et al.* 2009). The disadvantages associated with these traditional isolation devices are obvious in terms of ageing and durability, strict maintenance requirements, long-term performance and residual displacement (Dolce *et al.* 2000; Dion *et al.* 2011). Shape memory alloys (SMAs), which are characterized by their super-elasticity and energy dissipation, have the potential to be adopted within the bridge design and retrofit to improve the structural performance under earthquakes. The relevant studies are conducted within this study.

SMAs are generally associated with high strength, good fatigue and corrosion resistance besides the super-elasticity and energy dissipation; thus, can get rid of several drawbacks with respect to the traditional isolation devices (DesRoches *et al*. 2004; Song *et al.* 2006; Choi *et al.* 2005; Dezfuli and Alam 2014). Within the traditional bridge seismic design, steel is expected to yield for energy dissipation, which could result in a large residual deformation and hamper bridge functionality. To solve this problem, SMA could be implemented to resist the high seismic load without significant permanent residual deformations. In this paper, SMA is adopted within the highway bridges and is investigated to improve the seismic performance under earthquake hazard. The application of SMA within the bridge seismic mitigation process has been studied previously. SMA-cable/bar restrainer was used to replace the steel bar restrainer and was installed at in-span hinge or interface between the girder and abutment. Choi *et al*. (2005) and Dezfuli and Alam (2014) developed an isolation device that integrated SMA wires with rubber/elastomeric bearing to reduce the permanent residual deformation of the bridges under earthquakes. Xue and Li (2007) proposed a rubber bearing installed with pre-tensioning SMA-wires and applied it to a lattice shell structure for seismic mitigation. In this paper, the authors propose a novel frictional sliding bearing with SMA-cable, which fully takes advantages of the properties of SMAs, such as self-centering, super-elasticity, and energy dissipation. Another difference from the previous devices with application of SMA is that the SMA-cable is adopted instead of the wire to improve the re-centering capacity of SMA-wire. Additionally, this type of isolation device is more easily to be manufactured and installed. The effects of the proposed SMA-cable-based device on the bridge seismic performance are investigated.

To examine the feasibility of wide application of SMA within hazard mitigation process, it is necessary to investigate whether the higher initial cost can be paid off by considering the relative lower damage loss in a life-cycle context. Previously, the performance benefit associated with the SMA bridges has not been well recognized by the decision maker and life-cycle loss has not been emphasized within the decision-making process. Thus, the life-cycle engineering should be incorporated within the performance assessment process of bridges using SMA-based isolation device. In order to investigate the life-cycle performance, the bridge performance and damage consequence should be identified firstly. Pacific Earthquake Engineering Research (PEER) Center has developed a performance-based assessment approach considering repair loss, downtime, and fatalities. This approach is adopted within this study to compare the performance of different structural systems in a life-cycle context. Life-cycle cost could act as an important performance indicator for the comparative study associated with different structural systems. Wen and Ang (1991) proposed a methodology to investigate the cost effectiveness of an active control system of structures under earthquakes in a life-cycle context; Kang and Wen (2000) used the life-cycle cost as a design objective to obtain the optimal design strategies for structures under single and multiple hazards; Padgett *et al*. (2010a) presented an approach to assess the cost-benefit ratio associated with different retrofit strategies in a life-cycle context; Dong and Frangopol (2017) investigated the life-cycle loss of highway bridges under multiple hazards considering the effects of climate change. To the best knowledge of the authors, the life-cycle concept and performance-based assessment have not been well incorporated within the assessment and comparison of conventional and novel systems using SMA. In this paper, the comparative assessment of the life-cycle performance of conventional and SMA bridges is conducted based on the performance-based engineering in a life-cycle context.

Nowadays, with respective to the hazard management of infrastructures, a widely-recognized indicator is resilience. Researchers have turned attention to the challenge of making infrastructure systems more resilient against devastating earthquakes. Resilience is related with the ability of a structural system to mitigate the hazard damage to infrastructures, society, , and economy. A methodology to evaluate the seismic resilience of conventional and novel bridges is obliged to meet current performance requirements. The seismic resilience associated with novel bridge systems with SMA is investigated in this paper and comparative assessment between the conventional and novel bridges is emphasized. Overall, a performance-based assessment framework that incorporates both resilience and life-cycle engineering is provided in this paper. This framework can be used for making comparison among different alternative designs and retrofit actions.

An approach to assess the seismic resilience and life-cycle performance of conventional and novel bridge systems is presented. The structural vulnerability of the conventional and novel structural systems is computed based on three-dimensional (3D) nonlinear finite element (FE) models. The seismic vulnerability of the structural components (e.g., columns and bearings) is studied by using nonlinear time-history analysis. The life-cycle loss associated with seismic hazard is computed considering the representative hazard scenarios that can happen during the investigated time interval and is incorporated within the performance-based design and assessment process. The life-cycle loss and resilience of these structural systems are computed in a life-cycle context. The proposed approach is illustrated on the conventional and novel bridge systems, which can be effectively used for the comparative assessment of different infrastructure systems to aid the application of emerging materials within the civil engineering.

2. Structural Seismic Vulnerability

In order to evaluate the life-cycle loss and resilience of the bridge under seismic hazard, the structural seismic vulnerability analysis should be conducted as indicated in Figure 1. Fragility curves are the commonly used method to quantify the probability of exceeding a certain damage state associated with structural components and systems under given hazard intensity. Fragility analysis of different types of bridges has been conducted by many studies (Shinozuka *et al.* 2000; Choi *et al.* 2004; Zhang and Huo 2009; Padgett *et al*. 2010b; Dong *et al.* 2013; Muntasir Billaha and Shahria Alamb 2015). The seismic demand should be computed to derive the analytical fragility curves based on the nonlinear time history analyses. The seismic demand assesses the engineering demand parameters as a function of a chosen ground motion intensity and can be quantified using appropriate seismic structural responses, such as deformation or ductility of vulnerable components. The peak ground acceleration (*PGA*), is typically used as a ground motion intensity indicator (Baker and Cornell 2006; Padgett and DesRoches 2007). Given the chosen seismic ground intensity, the median value of seismic demand can be computed as (Cornell *et al.* 2002)

$$EDP = a \cdot (IM)^b \quad \text{or} \quad \ln(EDP) = \ln a + b \ln(IM) \tag{1}$$

where *IM* is the ground motion intensity indicator and *a* and *b* are regression parameters derived from the analytical responses. A 3D FE model can be established using the SAP 2000

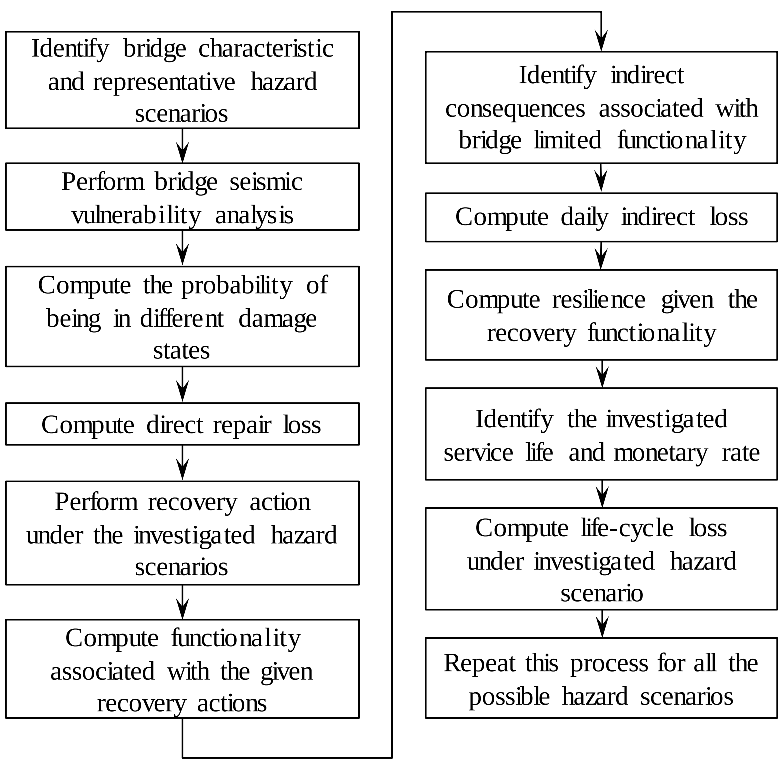

Figure 1. Flowchart for the performance-based assessment incorporating vulnerability, loss, resilience, and life-cycle loss

Table 1. Seismic damage states for RC columns and bearings

Bridge component	Damage indicator	Slight (DS = 1)	Moderate (DS = 2)	Major (DS = 3)	Collapse (DS = 4)
Column	Physical phenomenon	Cracking and spalling	Moderate cracking and spalling	Degradation without collapse	Failure leading to collapse
	Sectional ductility (μ_k) [a]	$\mu_k > 1$	$\mu_k > 2$	$\mu_k > 4$	$\mu_k > 7$
	Displacement ductility (μ_d) [b]	$\mu_d > 1.0$	$\mu_d > 1.2$	$\mu_d > 1.76$	$\mu_d > 4.76$
Bearing	Drift ratio (θ) [c]	$\theta > 0.007$	$\theta > 0.015$	$\theta > 0.025$	$\theta > 0.050$
	Displacement (δ) [a]	$\delta > 0$ mm	$\delta > 50$ mm	$\delta > 100$ mm	$\delta > 150$ mm

[a]: Choi *et al* 2004; [b]: Hwang *et al* 2001; and [c]: Yi *et al* 2007.

(Computers and Structures Inc. 2010) or OpenSees (McKenna *et al.* 2004) to assess the seismic demand. The standard deviation of ln(EDP) under given IM can be computed as (Baker and Cornell 2006)

$$\xi_{EDP|IM} = \sqrt{\frac{\sum_{i=1}^{n}[\ln(EDP_i) - (\ln a + b \ln IM_i)]^2}{n-2}} \tag{2}$$

where n is the number of the selected earthquake ground motions and EDP_i is the seismic response corresponding to the ith earthquake ground motion.

To obtain fragility curves of different components, it is necessary to specify the damage and capacity models. The damage states are usually discrete and are quantified by the designated thresholds of the chosen damage index DI to define different damage stages. Under a given ground motion intensity IM, the fragility curves can be expressed as (Cornell *et al.* 2002; Zhang and Huo 2009)

$$P[EDP - DI_i \geq 0 | IM] = 1 - \Phi\left(\frac{\ln(DI_i / aIM^b)}{\xi_{EDP|IM}}\right) \tag{3}$$

where $\Phi(.)$ is the standard normal distribution function and $\xi_{EDP|IM}$ is the standard deviation of the logarithmic distribution using Eq. (2). For highway bridges, reinforced concrete (RC) columns and bearings are the components that are susceptible to seismic damage. Sectional curvature ductility, displacement ductility, and residual displacement are often used as the seismic damage indicators for RC columns. Drift ratio, displacement, and shear strain can be used as the damage indicator for bearings. Four levels of the damage states namely slight, moderate, major, and collapse damages were proposed by HAZUS (2003). The definitions of these four levels corresponding to the chosen damage index *DI* are associated with RC column and bearings and are summarized in Table 1. Given the fragility curves, the probability of exceeding a certain damage state can be computed using Eq. (3). Subsequently, the probability of a structural component and system being in damage state *i* can be computed by the difference between the probabilities of exceedance of damage states *i* and *i*+1, where damage state *i*+1 is more severe than damage state *i*.

Given the fragility curves of the components, fragility curve of a bridge system can be developed accounting for the relationship between the vulnerable components and assessing structural performance as an overall system. Previous studies suggest that system fragility can be determined by considering the functionality of the bridges using a joint probabilistic seismic demand model associated with the vulnerable components. Other studies simply considered the column damage as the performance indicator of bridge system without considering other components. Nielson and DesRoches (2007) and Song and Kang (2009) computed the bridge fragility curves as an event that at least one component exceeds its corresponding damage state. Monte Carlo simulation method can be utilized to conduct the system fragility of bridges. This method, however, is time consuming. As an alternative method, the first-order reliability theory can be adopted to determine the upper and lower bounds on the system fragility. The lower bound is the maximum component fragility and the upper bound is a combination of the component fragilities. These bounds are expressed as follows (Nielson and DesRoches 2007)

$$\max_{k=1}^{m}[P(F_k)] \le P(F_{\text{sys}}) \le 1-\prod_{k=1}^{m}[1-P(F_k)] \tag{4}$$

where m is the number of the vulnerable component; $P(F_k)$ is the probability failure of the kth component; and $P(F_{\text{sys}})$ is the failure probability of the bridge system. Later, Zhang and Huo (2009) proposed a composite damage index to compute the system-level behavior of bridges under seismic hazard by using weighting factors. A weighting factor of 0.75 and 0.25 is assigned to the column and isolated device, respectively. Accordingly, the damage state of a bridge system can be computed as follows (Zhang and Huo 2009)

$$DS_{sys} = \begin{cases} \text{int}(0.75 \cdot DS_{col} + 0.25 \cdot DS_{bear}) & DS_{col} \ and \ DS_{bear} < 4 \\ 4 & DS_{col} \ or \ DS_{bear} = 4 \end{cases} \tag{5}$$

where DS_{col} and DS_{bear} represent the damage states of the column and the bearing, respectively.

3. SMA-Cable-Based Novel Bearing

Modeling of the proposed novel bearing using SMA is introduced in this section. SMA is a smart and novel material associated with shape memory and super-elasticity properties (Ozbulut *et al.* 2011). The shape memory effect is the ability of SMA to recover its original shape after deformation through a thermal cycling. The super-elasticity effect is described as the ability to recovery from a large strain due to the stress-induced martensitic phase transformations. To reflect the two properties of SMA, a flag-shaped hysteretic model (Tremblay *et al.* 2008) of SMA was developed as shown in Figure 2, in which E_A and E_M are the Young's moduli of the

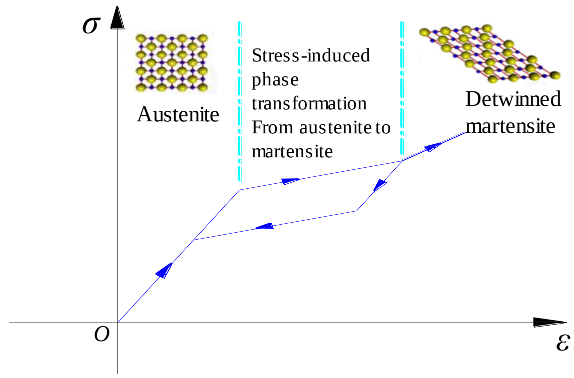

Figure 2. Constitutive hysteretic model of the Ni-Ti SMA material

SMA material at austenite and martensite phases, respectively. Given the cross-sectional area and the free displacements in both longitudinal and transverse directions of the SMA-cable, the strain-stress constitutive model of SMA-cable can be established using a one-dimension flag-shaped force-displacement model associated with the proposed isolation device.

The proposed novel seismically-isolated device consists of one frictional sliding bearing and two SAM-cable components as indicated in Figure 3(a). Some screwed holes exist on both the top and bottom plates of the frictional sliding bearing to aid the installation of the SMA-cable. The developed constitutive model of the proposed novel device is a parallel system as indicated in Figure 3(b), accounting for both the sliding effect associated with frictional sliding bearing and the energy dissipation and self-centering effects of the SMA-cable component. The frictional slide bearing is modeled using an elastic-perfectly plastic force-displacement constitutive model as indicated in Figure 3(b). The initial shear stiffness per unit length is represented by k_e and the sliding frictional force (F_s) of the frictional sliding bearing is given by

$$F_s = \mu N \tag{6}$$

where μ is frictional coefficient of the bearing component and N is the normal force acting on the bearing component. The SMA-cable component is modeled using a flag-shaped force-displacement constitutive model that is indicated in Figure 3(b). The flag-shaped model involves five parameters: u_0^s represents the gap of the SMA-cable component; k_0^s, k_1^s, k_2^s and k_3^s denote the axial tension stiffness per unit length of the slack SMA-cable component, the initial axial tension stiffness per unit length, the yielding axial tension stiffness per unit length, and the super-elastic stiffness per unit length of the SMA-cable component, respectively. The initial axial tension stiffness per unit length of the SMA-cable component can be expressed as

$$k_1^s = \frac{E_A A_S}{L} \tag{7}$$

where E_A is the initial Young's modulus of the SMA cable; A_s is the total cross-sectional area of all the SMA cables associated with the two SMA-cable components; and L is the length of the SMA-cable. The difference between the conventional and the SMA-cable-based bearings is that the conventional bearing does not have the SMA-cable components. Accordingly, the constitutive model of the conventional bearing is indicated in Figure 3(c).

4. Performance-Based Assessment and Resilience

4.1. Life-Cycle Loss Assessment

In order to investigate the benefit in collaboration with the SMA within the bridge design and hazard mitigation process, bridge performance assessment in a life-cycle context should be conducted. Life-cycle loss associated with conventional and novel bridge systems, as an important performance indicator, should be quantified to compare the performance between these two types of bridges considering different types of losses, e.g., direct and indirect loss (e.g., repair cost, downtime interruption, and injuries).

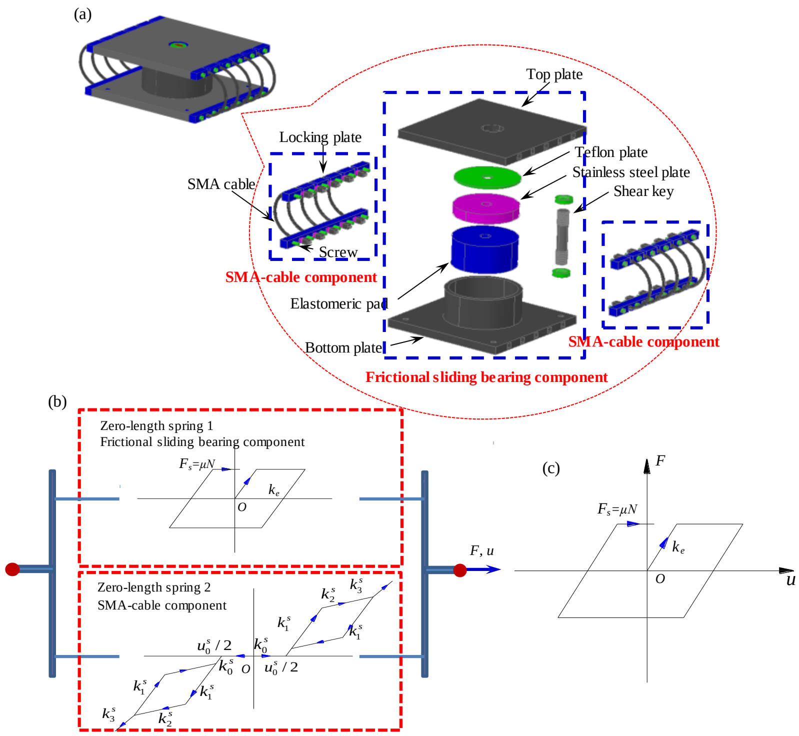

Figure 3. (a) Configuration of the modular SMA-cable-based bearing, (b) constitutive model of the novel bearing with frictional sliding bearing and SMA-cable component, and (c) constitutive model of the conventional bearing loss

The performance-based engineering is adopted within the performance quantification process. Basically, the performance-based performance under hazards can be assessed using the following steps: hazard analysis, structural analysis, damage analysis, and loss analysis. The detailed flowchart regarding the performance-based assessment is shown in Figure 1. In order to assess the seismic loss, the investigated hazard scenarios should be identified. The selected hazard scenarios should be able to represent the earthquake intensity at the location of the investigated bridge incorporating both the frequent lower magnitude and the larger magnitude earthquakes with low probability of occurrence. For instance, the seismic intensity can be classified as lower, upper, and severe cases (Ataei *et al.* 2017). The lower level seismic event refers to a relatively small but frequent earthquake that can happen with a reasonable likelihood within the service life of the bridge. The design service life for a bridge is usually 75 years.

Accordingly, lower level ground motion could be determined as a 50% probability of exceedance within the life of a bridge and this is associated with a 120-year return period. The upper level earthquake event represents a large with a relatively low probability of occurrence within the service life. For instance, the upper level earthquake scenario could refer to a 10% probability of exceedance within the service life and is with a return period of 715 years approximately. A severe earthquake represents a high intensity ground motion with a rare probability of occurrence within the service life of a bridge. Herein, the severe earthquake is assumed to with a 5% probability of exceedance in 75 years and is associated with approximate 1450-year return period earthquake scenario. Overall, given the prescribed investigated hazard levels, the selected seismic scenarios can be identified accordingly.

The loss of bridges under the selected earthquake scenarios is investigated herein. Given the fragility curves, the probability of bridges being in different damage states could be computed. Subsequently, based on the theorem of total probability, the loss is the sum of consequences weighted with the probabilities of having these consequences. The expected annual loss under the given the occurrence of the hazard can be computed as

$$l_i = \sum_{DS} C_{DS} \cdot P_{DS|IM} \tag{8}$$

where C_{DS} is the consequence associated with the given damage state of the bridge and $P_{DS|IM}$ is the conditional probability of a damage state given a hazard intensity. The direct and indirect consequences associated with bridge being in different damage states are investigated. The repair cost associated with a given damage state is assumed proportional to the rebuilding cost of the bridge (Stein *et al.* 1999) and is

$$C_{REP} = RCR \cdot c_{reb} \cdot W \cdot L \tag{9}$$

where RCR is the repair cost ratio for a damaged bridge; c_{reb} is the rebuilding cost per square meter (USD/m^2); W is the bridge width (m); and L represents the bridge length (m). The repair cost is usually regarded as direct cost. Indirect cost could also be incorporated within the consequence evaluation procedure and can be much larger than the direct cost. Once the bridge is damaged, the drivers are forced to follow the detour route. The cost associated with running vehicles on detour is (Stein *et al.* 1999; Dong and Frangopol 2015)

$$C_{RUN} = \sum_{i=1}^{t_{IL}} \left[c_{Run,car} (1 - \frac{T}{100}) + c_{Run,truck} \frac{T}{100} \right] D_l \cdot ADTD \tag{10}$$

where $c_{Run,car}$ and $c_{Run,truck}$ are the costs for running cars and trucks per unit length (USD/km), respectively; t_{IL} is the time interval until the bridge reaches full functionality (e.g., days); D_l is the length of detour (km); $ADTD$ is the average daily traffic to detour; and T represents the average daily truck traffic ratio. The monetary time loss for users and goods traveling through the detour and damaged link can be expressed as (Stein *et al.* 1999; Dong *et al.* 2013)

$$C_{TL} = \sum_{i=1}^{t_{IL}} \left[c_{AW} O_{car} (1 - \frac{T}{100}) + (c_{ATC} O_{truck}) \frac{T}{100} \right] \cdot \left[ADTD \cdot \frac{D_l}{S} + ADTE \cdot (\frac{l_l}{S_D} - \frac{l_l}{S_0}) \right] \tag{11}$$

where c_{AW} is the wage per hour (USD/h); c_{ATC} is the compensation per hour (USD/h); c_{goods} is the time value of the goods transported in a cargo (USD/h); $ADTE$ is the average daily traffic remaining on the damaged link; O_{Car} and O_{Truck} are the average vehicle occupancies for cars and trucks, respectively; l_l is the route segment (i.e., link) containing the bridge (km); S_0 and S_D represent the average speed on the intact link and damaged link (km/h), respectively; and S represents the average detour speed (km/h).

Given the annual loss under the selected hazard, the loss of the bridge within the investigated time interval can be computed. Given the occurrence of earthquake as a Poisson process, the total seismic loss in a life-cycle context can be computed as

$$Lt_i(t_{\text{int}}) = \sum_{i=1}^{N(t_{\text{int}})} l_i(t_k) \cdot e^{-\gamma t_k} \tag{12}$$

where t_{int} is the investigated time interval (e.g., years); $N(t_{int})$ is the number of hazard events that occur during the time interval; $l_i(t_k)$ is the expected annual hazard loss at time t_k; and γ is the monetary discount rate. Given $N(t_{int}) = \lambda_f \times t_{int}$, the total expected life-cycle loss can be computed as (Wen and Kang 2001; Dong and Frangopol 2016)

$$E[Lt_i(t_{\text{int}})] = \frac{\lambda_f \cdot E(l_i)}{\gamma} \cdot (1 - e^{-\gamma \cdot t_{\text{int}}}) \tag{13}$$

where $E(l_i)$ is the expected value of annual loss l_i given a seismic event. Given all the investigated hazard scenarios, the total life-cycle loss associated with all the investigated seismic scenarios is

$$E[TLt_i(t_{\text{int}})] = \sum_{i=1}^{N_{sc}} \frac{\lambda_i \cdot E(l_i)}{\gamma} \cdot (1 - e^{-\gamma \cdot t_{\text{int}}}) \tag{14}$$

where N_{sc} is the number of hazard scenarios under investigation.

4.2. Resilience

Resilience, as another important structural performance indicator under extreme event, is defined as the ability of a civil infrastructure system to maintain its functionality and return to normality after an extreme event, which depends on the functionality level and recovery patterns. The functionality of a bridge can be defined as the ability of opening traffic after an extreme event. Different functionality levels should be considered for emergency response and post-earthquake recovery period. In the emergency response planning, it is of great importance to identify whether the bridge located on a link is still available to transfer the resources to the disaster area. In the post-earthquake recovery phase, the functionality associated with the bridge under hazard event can be defined as closed, limited use, and open. Based on the recovery pattern, the resilience of the bridge under an extreme event can be computed. One of the most widely adopted approaches to quantify the resilience is (Cimellaro *et al.* 2010; Frangopol and Bocchini 2011)

$$R_{Resi} = \frac{1}{\Delta t_r} \int_{t_0}^{t_0+\Delta t_r} Q(t)dt \tag{15}$$

where $Q(t)$ is the functionality of a bridge under recovery function at time t (e.g., days); t_0 is the investigated point in time; and Δt_r is the investigated time interval (e.g., days, months). The shape of the performance restoration curve is related with the repair and recovery efforts. In order to quantify the resilience, the functionality $Q(t)$ should be identified. Generally, the bridge functionality can be assessed by mapping the bridge damage state to a value between 0 and 1.0 (Dong and Frangopol 2015). For instance, the value 0 is associated with collapse of the bridges. Given the functionality associated with different damage states, the expected functionality can be computed as (Dong and Frangopol 2015)

$$Q = \sum_{i=1}^{5} FR_i \cdot P_{DS_i|IM} \tag{16}$$

where FR_i is the functionality ratio associated with damage state i. Herein, the following scenarios are considered: immediate access, weight restriction, one lane open only, emergency access only, and bridge closed represent. These functionality categories are mapped to a functionality level between 0 and 1.0 as $Func > 0.9$, $0.6 < Func \leq 0.9$, $0.4 < Func \leq 0.6$, $0.1 < Func \leq 0.4$, and $Func \leq 0.1$, respectively (Dong and Frangopol 2015). In HAZUS (ATC 1999), the bridge functionality restoration process was modeled by a normal cumulative distribution function corresponding to the four bridge damage states: slight, moderate, major, and complete (collapse); Padgett and DesRohes (2007) investigated bridge functionality recovery based on web-based survey; and Decò *et al.* (2013) proposed a probabilistic approach for calculating the resilience of bridges. Then, given functionality under the recovery pattern, the resilience is computed using Eq. (15).

5. Illustrative Example

The presented approach is applied to a reinforced concrete (RC) bridge with the proposed SMA-cable-based bearing. The relevant performance indicators, such as fragility curves, life-cycle loss, and resilience are investigated and compared with the conventional bridge. This study can aid the application and development of emerging materials within the civil engineering.

5.1 Bridge Description and Modelling

The bridge investigated herein is a continuous RC bridge with two equal spans (i.e., 20 + 20 *m*). The geometry of the box girder, column, and abutment is shown in Figure 4. As indicated, the

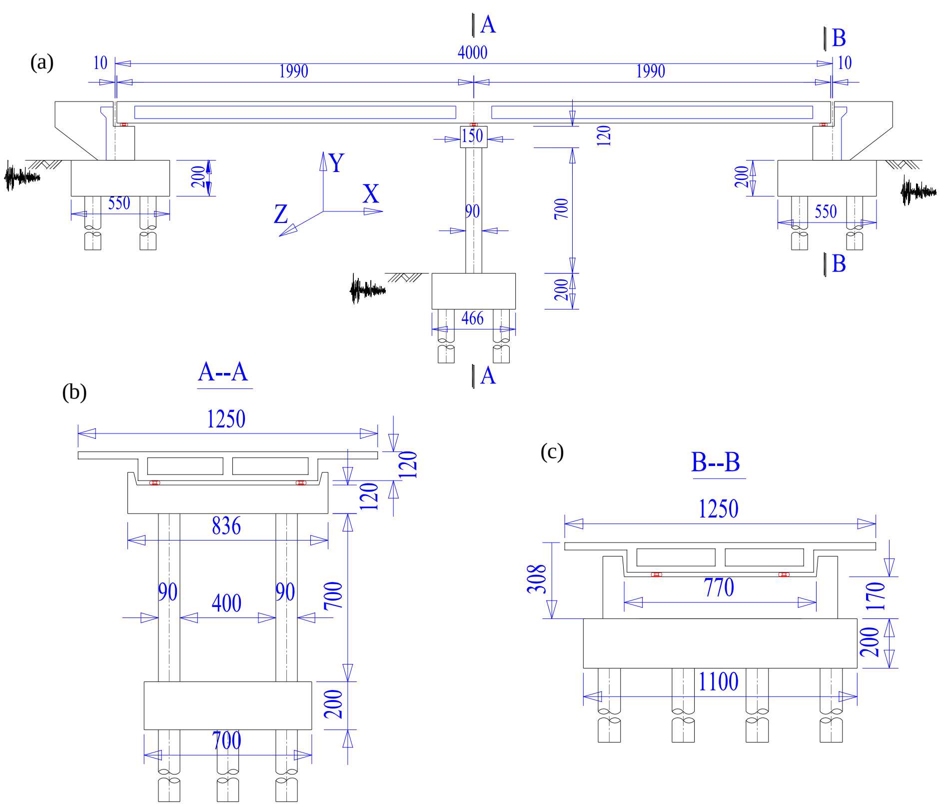

Figure 4. (a) Configuration for the investigated continuous RC bridge (unit: cm), (b) elevation view, and (c) section view of the bridge

height and the width of the RC two-box girder are 1.2 *m* and 12.5 *m*, respectively. The clear height of the RC column is 7.0 *m*, and the cross section of the RC column is 0.9 *m* × 0.9 *m*. The longitudinal and transverse reinforcement ratios of the RC column are 0.024 and 0.00251, respectively. The compressive strength of the concrete used in the column is 30.0 MPa and the yield strength of the reinforcement is 280.0 MPa. Based on the pushover analysis, the relationship between the bending moment and curvature of the RC column section is shown in Figure 5(a), which could be represented by a bilinear curve. Accordingly, the yielding bending moment and the curvature are 2970.1 kN.m and 0.00461/m, respectively.

The seismic vulnerability of the conventional and novel bridges with SMA-cable bearings is investigated. The schematic FE model of the continuous RC bridge is shown in Figure 5(b). For the conventional RC bridge, two conventional expansion bearings are placed on the top of abutment and two conventional fixed bearings are placed on the top of the bent cap. As an example, the constitute model of the expansion bearing is indicated in Figure 3(c). The yielding strength (F_s) of the expansion bearing is computed as the product of the frictional coefficient (μ) and the normal force (N) acting on the bearing. The initial elastic stiffness per millimeter (k_e) and the frictional coefficient are 123 kN/mm and 0.2 (Mander *et al.* 1996). With respect to the novel isolated bridge, two SMA-cable-based expansion bearings are placed on the top of abutment and two SMA-cable-based fixed bearings are placed on the top of the bent cap. The SMA-cable-based fixed and expansion bearings are modeled by two zero-length spring elements in parallel as illustrated in Figure 3(b). The initial gap (u_0^s) is 50 *mm* and the initial axial tension stiffness per unit length (k_1^s) of the SMA-cable component is 72.7 kN/mm. The ratio between the yielding axial tension stiffness per unit length (k_2^s) and k_1^s is 0.015. The ratio between the super-elastic tension stiffness per unit length (k_3^s) and k_1^s is 1.0. The SMA-cable-based bearing is used here to enhance the seismic performance of bridge under seismic hazard.

The RC columns are modeled by displacement-based nonlinear fiber elements accounting for the nonlinear characteristics. The constitutive behavior of the reinforcing steel is represented by a uniaxial Menegotto-Pinto constitutive model (Menegotto and Pinto 1973; Barbato and Conte 2006). The uniaxial Kent-Scott-Park concrete model (Scott *et al.* 1982) is used to model the unconfined and confined concrete. The soil-structure interaction (SSI) effect of the soil-abutment-pile-foundation is modeled by several zero-length spring elements in parallel (Maragakis *et al.* 1991). Specifically, a tri-linear hysteretic model is assigned to a zero-length spring element to simulate the dynamic mechanism of the SSI between the soil and abutment. The superstructure and RC abutment are modeled by using linear elastic beam-column elements.

5.2 Seismic Vulnerability Assessment

In order to conduct the nonlinear time-history analysis, a set of 88 ground motion records is selected from Pacific Earthquake Engineering Research Center Ground Motion Database (PEER 2013). This suite of selected records covers a wide range of magnitude. The seismic performance of SMA-cable-based bearings and the RC columns, as the most vulnerable components, is investigated and median values corresponding to their appropriate seismic demands are computed using Eq. (1). For the RC column within the conventional bridge, taking the PGA and maximum curvature ductility as the seismic intensity and demand parameter, the two constants a and b can be obtained based on the linear regression and they are 6.003 and 1.960, respectively, as indicated in Figure 6(a). Similarly, the values of a and b associated with the columns of the novel bridge are 2.167 and 2.033, respectively, as indicated in Figure 6(b). The relevant regression parameters associated with conventional and proposed novel bearings can also be

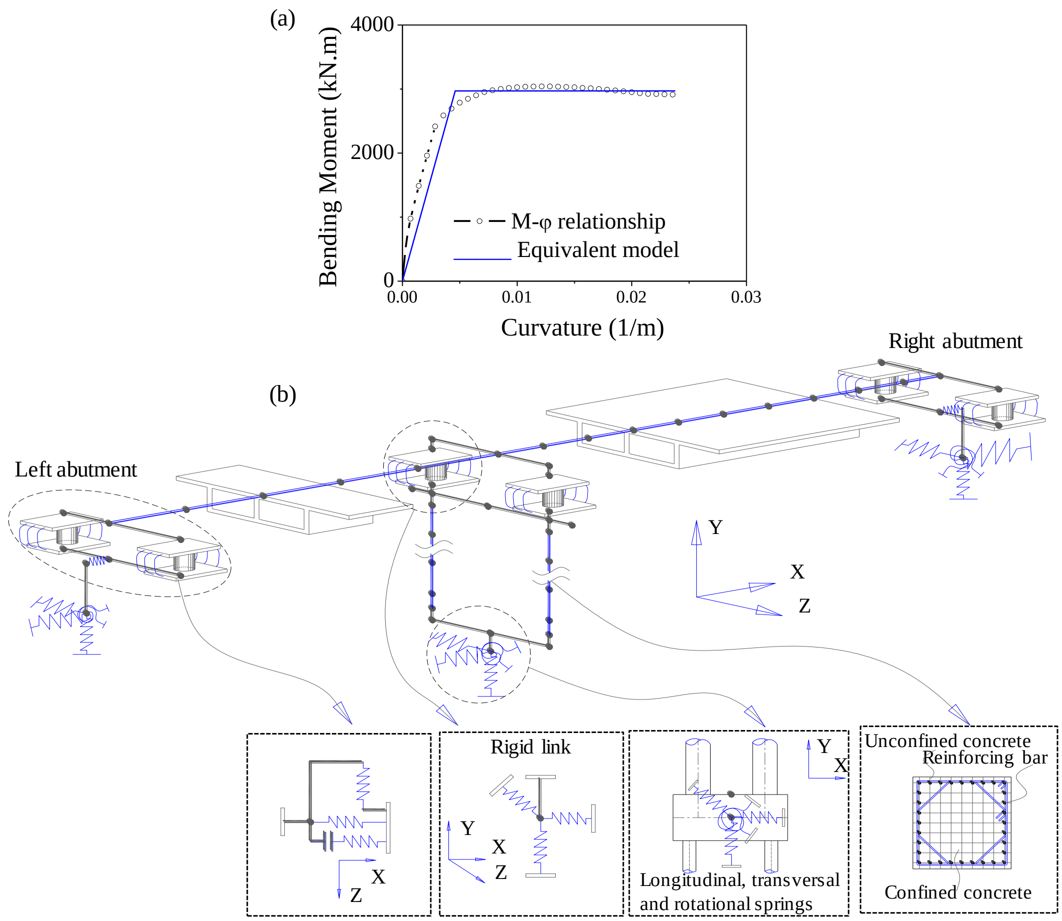

Figure 5. (a) Bending moment vs. curvature of the section at the bottom of the RC column and (b) nonlinear FE model of the investigated bridge

obtained. For the conventional bearing, these two constants *a* and *b* are 0.1333 and 1.401, respectively, as shown in Figure 6(c). For the novel SMA-cable-based bearing, *a* and *b* are 0.0684 and 1.636, respectively, as shown in Figure 6(d).

Given the seismic demand, the fragility curves of the RC column and bearing with and without using SMA are obtained. The parameters used for the quantification of different damage states of the RC column and bearing are indicated in Table 1. The fragility curves can be computed using Eq. (3). Accordingly, Figure 7(a) shows the fragility curves associated with four damage states of the RC columns with conventional bearings and SMA-cable-based bearings. As indicated, under a given ground motion intensity, the damage probabilities of the RC column of the conventional bridge are much larger than those of the RC column within the isolated bridge using SMA-cable-based bearings. Thus, the SMA-cable-based bearing can improve the structural performance of the RC columns significantly. For instance, given the *PGA* = 1.0 *g*, the probabilities of exceeding the four damage states of the RC column within the novel bridge

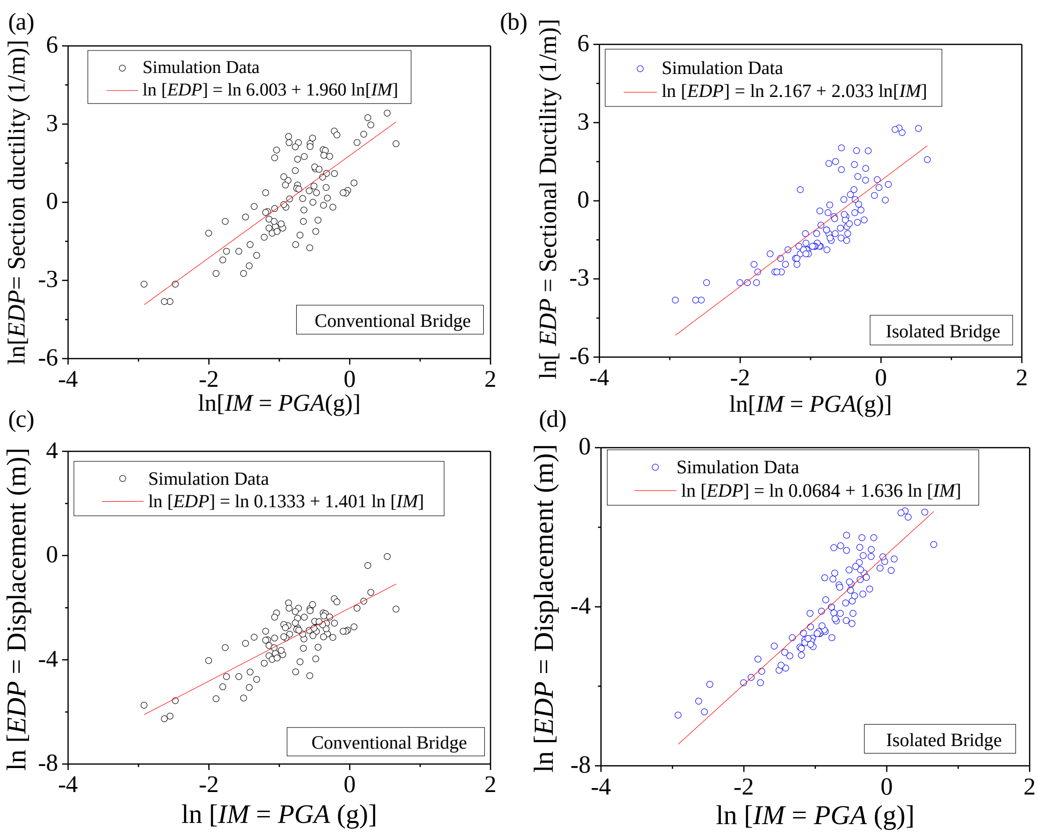

Figure 6. Relationship of logarithmic *EDP* against logarithmic *IM* of the RC column (a) Conventional bridge, (b) novel bridge with SMA, and relationship of logarithmic EDP against logarithmic IM of the bearings (c) conventional bridge, and (d) novel bridge with SMA

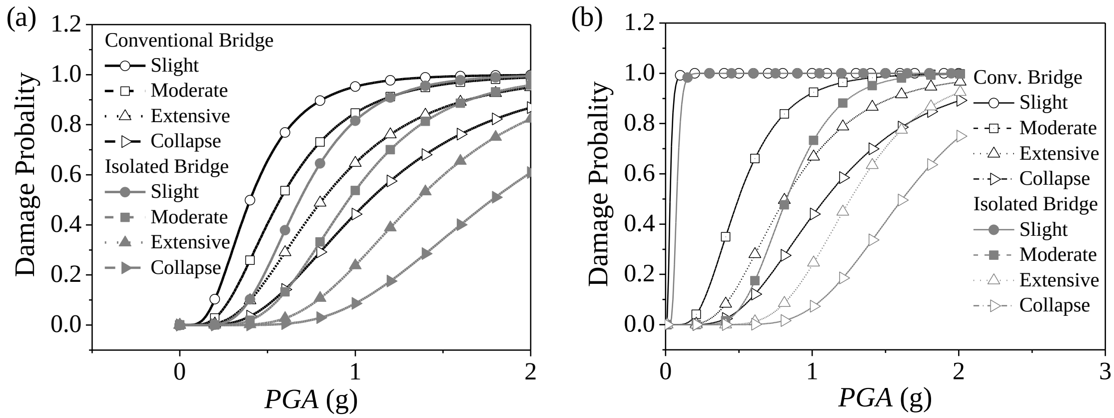

Figure 7. Fragility curves of (a) RC columns and (b) bearings the conventional and isolated novel bridges with SMA

system are 85.7%, 63.5%, 36.8% and 19.4% of those of the conventional bridge. The fragility curves of the conventional and SMA-cable-based bearings are indicated in Figure 7(b). It can be concluded that the damage probabilities of the conventional bearing associated with four damage states are larger than those of the SMA-cable-based bearings. Similarly, the SMA-cable-based bearing can improve the performance of the bearings under earthquakes significantly.

Given the fragility curves associated with different components, the system-level fragility curve can be obtained. The system failure model proposed by Nielson and DesRoches (2007) is

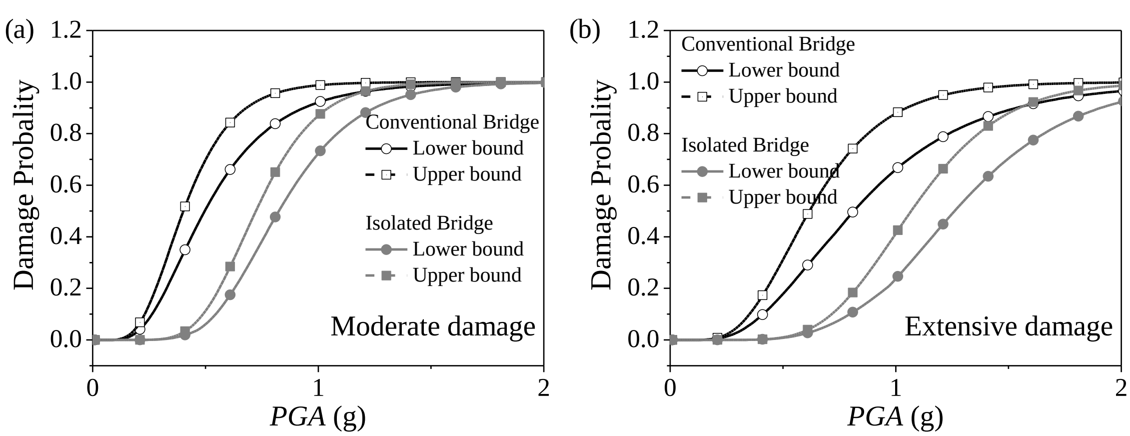

Figure 8. System fragilities for (a) moderate damage and (b) major damage of conventional and novel bridges

used to compute the system-level bridge fragility curve considering the seismic performance of the columns and bearings. As indicated in Eq. (4), the fragility curves of the bridge system at each damage state compose two parts, i.e., upper and lower bounds. The upper bound indicates the combination of the component fragilities while the lower bound represents the maximum component fragility. The fragility curves associated with moderate and major damage states are plotted in Figure 8. As indicated, the SMA-cable-based bearing can improve the structural performance of the bridge system significantly. At moderate damage state, the upper and lower bounds for the conventional bridge are much higher than those for the novel bridge. For instance, given the PGA = 1.0 g, the upper and lower bounds of the novel bridge system exceeding moderate damage are approximately 88.0% and 78.5% of those of the conventional bridge. With respect to the extensive damage state, given the PGA = 1.0 g, the upper and lower bounds of the novel bridge system are approximate 21.5% and 18.9% of those of the conventional bridge. Thus, the SMA cable-based bearing has a larger effect on the bridge performance with respect to a severe damage state.

5.3 Resilience Assessment

The resilience of the conventional and novel bridges is assessed in this section, in which the functionality of bridges considering different damage states should be identified firstly. Herein, the following scenarios are considered: immediate access, weight restriction, one lane open only, emergency access only, and bridge closed; these functionality categories are mapped to a functionality level between 0 and 1.0 as $Q(t) > 0.9$, $0.6 < Q(t) \leq 0.9$, $0.4 < Q(t) \leq 0.6$, $0.1 < Q(t) \leq 0.4$, and $Q(t) \leq 0.1$, respectively (Dong and Frangopol 2015). Given the hazard intensity, the functionality of the bridges after the earthquake is computed using Eq. (16). Given the lower and upper bounds associated with different damage states, the bridge fragility curve can be obtained

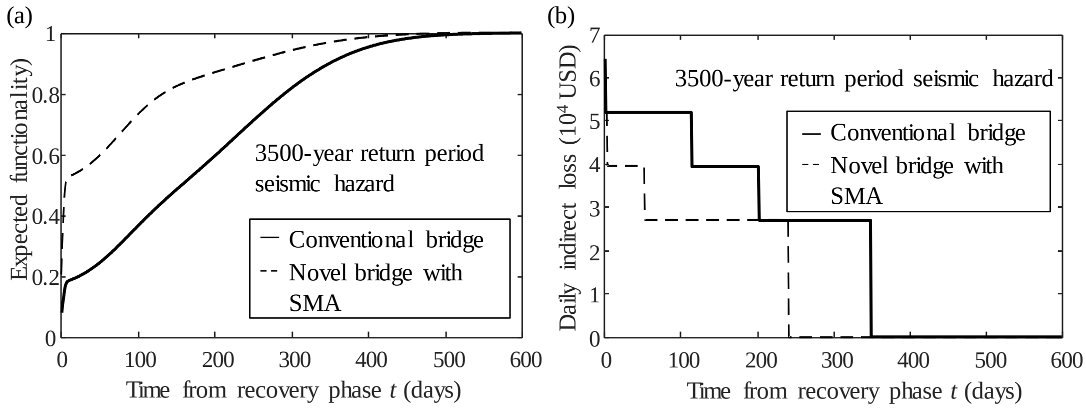

Figure 9. (a) Expected functionality of the bridge from the recovery phase and (b) daily indirect loss associated with the novel and conventional bridges under the given hazard

as the average of these two bounds. The four hazard scenarios are investigated herein, which refer to the 120, 715, 1450, and 3500-year return period earthquakes. For illustrative purpose, two locations are selected in this study: Nutbush, Tennessee and Los Angeles, California. Hazard curve parameters for Nutbush and Los Angeles are based on the United States Geological Survey (2017). The *PGA*s with return period of 120, 715, 1450, and 3500-year at Nutbush are 0.061, 0.337, 0.528, and 0.809 *g*, respectively. With respect to the Los Angeles, the relevant *PGA*s are 0.2774, 0.659, 0.860, and 1.157 *g*, respectively. Given the seismic intensity and fragility curve, the probabilities of the bridge being in different damage states can be obtained, which act as the input for Eq. (16). The expected residual functionalities of the novel bridge located at Los Angeles under four selected seismic intensities are 0.747, 0.582, 0.400, and 0.203, respectively. With respect to the novel bridge located in Nutbush, the residual functionalities are 0.936, 0.743, 0.687, and 0.445, respectively. By comparison, the seismic intensity associated with different locations of bridge can affect the functionality significantly. Also, the functionality of the conventional bridge at the Los Angeles is also computed. The residual functionality of the conventional bridge under the investigated four return period earthquakes are 0.664, 0.258, 0.1519, and 0.0772, respectively.

Given the functionality of the bridges after the earthquake, the resilience of the bridge can be computed using Eq. (15). Herein, the recovery path is based on ATC (1999). Accordingly, the bridge functionality restoration process is modeled by a normal cumulative distribution function corresponding to each of the four bridge damage states: slight, moderate, major, and complete (collapse). The approach developed by ATC is adopted within this paper and any other models can also be easily incorporated within the computational process. Under the recovery strategies, the functionality of the bridge can recovery to a desirable level. Under the investigated 3500-year return period earthquake and recovery actions, the functionality of the bridge is shown in Figure 9(a). As indicated, the functionality of the damaged bridge increases with time and there exists a significant difference between the conventional and novel bridges. Then, based on Eq. (15), the resilience of the conventional and novel bridges is computed. Given Δt_r = 300 days, the resilience of the novel bridges located in Los Angeles under the four seismic hazard intensities is 0.996, 0.975, 0.920 and 0.770, respectively. The resilience of the bridges under the investigated earthquake scenarios is shown in Table 2. By comparing these values, the resilience of the bridge can be increased by 46.5% of the case of adopting SMA novel system under 1450-year seismic event. As indicated, the performance benefit of resilience associated with SMA increases with a larger investigated hazard intensity. It means that the SMA is more beneficial for the bridges that located within the seismic active zones with a higher hazard intensity.

Table 2. Resilience of the conventional and novel bridges located in different regions under different hazard intensities

Return Period (years)	Los Angeles, CA		Nutbush, TN	
	Conventional Bridge	Novel Bridge	Conventional Bridge	Novel Bridge
120	0.984	0.996	0.996	0.997
715	0.767	0.975	0.967	0.996
1450	0.628	0.920	0.863	0.991
3500	0.479	0.770	0.661	0.938

5.4 Life-Cycle Loss Assessment

In order to compute the life-cycle loss, the annual loss given the occurrence of the seismic scenarios should be computed. Based on the fragility curves obtained previously, the probabilities of the bridge being in different damage states are quantified. Then, given the consequences associated with different damage states, the direct and indirect costs can be quantified using Eqs. (9) - (11). Accordingly, the direct repair cost associated with the damaged bridge is computed using Eq. (9). The expected repair loss of the bridge using SMA at Los Angeles under the investigated four earthquake scenarios are 1.436×10^5, 2.737×10^5, 4.699×10^5, and 8.013×10^5 USD, respectively. The indirect loss associated with the bridge considering partial functionality is computed using Eqs. (10) and (11). The parameters used in these equations are indicated in Table 3. The time-variant daily indirect loss is shown in Figure 9(b). Once the functionality of the bridge is completely restored, the daily indirect loss reaches zero at the end of the investigated time interval. The total indirect loss of the damaged bridge is the sum of the daily loss. The total indirect losses associated with conventional and novel bridges under the four investigated hazard scenarios are computed. The total indirect loss of the bridge using SMA at Los Angeles under the investigated four earthquake scenarios are 2.698×10^4, $1.204 \times$

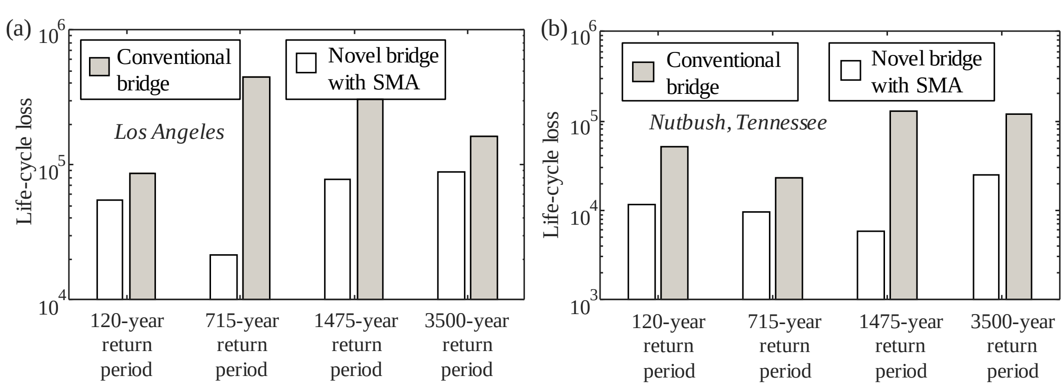

Figure 10. Life-cycle loss associated with the conventional and novel bridges under different hazard scenarios at (a) Los Angeles, CA and (b) Nutbush, TN

10^5, 2.454.699 × 10^6, and 7.188 × 10^6 USD, respectively. By comparing, the indirect loss is much larger than the direct repair loss as the seismic intensity increases.

Table 3. Parameters associated with the consequence evaluation

Random variables	Notation	Value
Average daily traffic	ADT	19750
Daily truck traffic ratio	T	13%
Length of link (km)	l_l	6
Detour additional distance (km)	D_l	2
Vehicle occupancies for cars	O_{car}	1.5
Vehicle occupancies for trucks	O_{truck}	1.05
Rebuilding costs ($/m^2)	c_{reb}	2306
Compensation for truck drivers ($/h)	c_{ATC}	29.87
Operating costs for cars ($/km)	$c_{Run,car}$	0.4
Operating costs for trucks ($/km)	$c_{Run,truck}$	0.57
Wage for car drivers ($/h)	c_{AW}	11.91
Detour speed (km/h)	S	50
Link speed (km/h)	S_0	80

Then, the expected loss within the life-cycle of the bridge is assessed using Eq. (13). Considering the investigated four earthquake scenarios, the life-cycle loss of the conventional and novel bridges located in Los Angeles, CA, is shown in Figure 10(a). As indicated, the SMA-

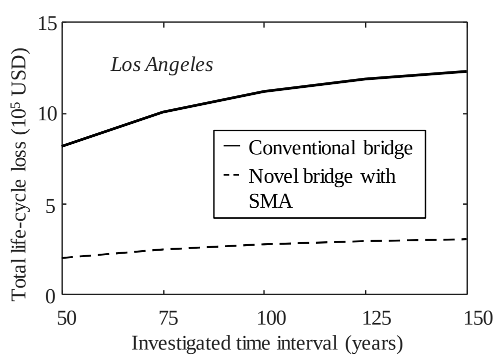

Figure 11. Effect of investigated time intervals on the life-cycle loss of the conventional and novel at Los Angeles, CA

cable based bearing can reduce the life-cycle loss significantly compared to the bridge with the conventional bearing, especially for the 715-year return period earthquake scenario. Similarly, the life-cycle losses of the conventional and novel bridges located in Nutbush, TN, are computed and indicated in Figure 10(b). As indicated, there exists a significant difference between these two types of bridges. The SAM cable-based bearing has a larger effect on the loss reduction associated with 1475-year return period earthquake. The effects of the investigated time interval on the life-cycle loss are also assessed within the computational process. Figure 11 shows the profiles of the life-cycle loss of the conventional and novel bridges located in Los Angeles under different time intervals. As the results indicated, the bridge life-cycle loss increases over time and the difference between the losses of conventional and novel bridges increases with the increase of the time interval.

6. Conclusions

This paper presents an approach to assess the life-cycle loss and resilience of conventional and novel structural systems with SMA cable-based bearings in order to evaluate the benefit associated with the adoption of this novel bearing system. The fragility curves associated with the conventional and novel bridges with SMA were evaluated by using nonlinear time-history analysis. Life-cycle loss and resilience under the investigated hazard scenarios were assessed, taking into account the direct and indirect loss and hazard recovery pattern. The proposed novel isolation device was applied to a continuous RC bridge.

The following conclusions can be drawn.

1. The effect of SMA-cable based bearing on the seismic performance of a highway bridge was investigated by using time history analysis. The proposed novel isolation device can

improve the seismic performance of the bridge significantly. Thus, the bridges with the proposed SMA devices proved to be effective considering the structural performance and the relevant loss associated with bridge failure.

2. The seismic loss of the bridges within the investigated time interval was assessed and compared with the novel and conventional bridges. The indirect loss is highly related with the investigated hazard intensity. Indirect loss could be much larger than the direct loss, specifically for the investigated seismic scenario with a relatively low probability of occurrence. As can be concluded from the results, the life-cycle loss of the bridge using the novel isolation device with SMA can be reduced significantly. The investigated time interval can affect the life-cycle loss significantly and different conclusions can be obtained associated with different investigated time horizon.
3. The contribution of the hazard scenarios on the life-cycle loss depended not only on the hazard occurrence rate but also the annual loss given the occurrence of the investigated hazard scenarios. In order to cover a comprehensive performance assessment content, different hazard scenarios should be chosen within the evaluation process. The performance benefit of resilience associated with SMA increases with a larger investigated hazard intensity. SMA is more beneficial for the bridges that located within the seismic active zones with a high hazard intensity.
4. The resilience of the conventional and novel bridge systems was assessed in this study. The functionality and probability of the bridge in different performance levels were computed to aid the assessment of resilience. The investigated seismic intensity can affect the resilience significantly. The difference of the resilience between the conventional and novel bridge systems increases with the increase associated with the investigated hazard scenario.

5. This paper provided a decision-making tool for the application of novel materials within the structural seismic design process. The comparative seismic vulnerability, life-cycle loss, and resilience of different bridge systems were investigated. The proposed SMA cable-based bearings can improve the seismic performance of the bridge significantly in a long-term time interval.

Acknowledgement

The study has been supported by The Hong Kong Polytechnic University under Start-Up Fund number 1-ZE7Q and the natural science foundation of the Shanghai Pujiang Program under grant number 16PJ1409600 are gratefully acknowledged. The opinions and conclusions presented in this paper are those of the authors and do not necessarily reflect the views of the sponsoring organizations.

References

ATC (1999). *Earthquake damage evaluation data for California*. Technical report ATC-13. Applied Technology Council.

Ataei, H., Mamaghani, M., and Lui, E.M. (2017). Proposed framework for the performance-based seismic design of highway bridges. *Structures Congress 2017*, April 04, 2017, Denver, CO.

Baker, J.W., and Cornell, C.A. (2006). *Vector-valued ground motion intensity measures for probabilistic seismic demand analysis*. PEER report 2006.08. Berkeley: Pacific Earthquake Engineering Research Center, University of California Berkeley.

Barbato, M., and Conte, J.P. (2006). Finite element structural response sensitivity and reliability analysis using smooth versus non-smooth material constitutive models. *International Reliability Safety*, 1, 3-39.

Bhuiyan, A.R., Okui, Y., Mitamura, H., and Imai, T. (2009). A rheology model of high damping rubber bearings for seismic analysis: identification of nonlinear viscosity. *International*

Journal of Solids Structures, 46(7-8), 1778-1792.

Choi, E., DesRoches, R., and Nielson, B. (2004). Seismic fragility of typical bridges in moderate seismic zones. *Engineering Structures*, 26, 187–199.

Choi, E., Nam, T., and Cho, B.S. (2005). A new concept of isolation bearings for highway steel bridges using shape memory alloys. *Canada Journal of Civil Engineering*, 32, 957-967.

Cimellaro, G.P., Reinhorn, A.M., and Bruneau, M. (2010). Seismic resilience of a hospital system. *Structure and Infrastructure Engineering*, 6, 127–144.

Cornell, A.C., Jalayer, F., and Hamburger, R.O. (2002). Probabilistic basis for 2000 SAC federal emergency management agency steel moment frame guidelines. *Journal of Structural Engineering*, 128, 526-532.

Decò, A., Bocchini, P., and Frangopol, D.M. (2013). A probabilistic approach for the prediction of seismic resilience of bridges. *Earthquake Engineering & Structural Dynamics*, *42*(10), 1469-1487.

DesRoches, R., McCormick, J., and Delemont, M. (2004). Cyclic Properties of Superelastic Shape Memory Alloy Wires and Bars. *Journal of Structural Engineering*, 130(1), 38-46.

Dion, C., Bouaanani, N., Tremblay, R., Lamarche, C-P., and Leclerc, M. (2011). Real-time dynamic substructuring testing of viscous seismic protective devices for bridge structures. *Engineering Structures*, 33(12), 3351-3363.

Dong, Y., Frangopol, D.M., and Saydam, D. (2013). Time-variant sustainability assessment of seismically vulnerable bridges subjected to multiple hazards. *Earthquake Engineering and Structural Dynamics*, 42(10), 1451-1467.

Dolce, M., Cardone, D., and Marnetto, R. (2000). Implementation and testing of passive control devices based on shape memory alloys. *Earthquake Engineering and Structural Dynamics*, 29(7), 945-968.

Dong, Y., and Frangopol, D.M. (2015). Risk and resilience assessment of bridges under mainshock and aftershocks incorporating uncertainties. *Engineering Structures*, 83, 198-208.

Dong, Y., and Frangopol, D.M. (2016). Probabilistic time-dependent multihazard life-cycle assessment and resilience of bridges considering climate change. *J. Perform. Constr. Facil.*, 30(5), 04016034, 1-12.

Frangopol, D.M., and Bocchini, P. (2011). Resilience as optimization criterion for the rehabilitation of bridges belonging to a transportation network subjected to earthquake. *SEI-ASCE 2011 Structures Congress*. April 14–16, Las Vegas, NV.

Ghobarah, A., and Ali, H.M. (1990). Seismic design of base-isolated highway bridges utilizing lead-rubber bearings. *Canada Journal of Civil Engineering*, 17(3), 413-422.

HAZUS (2003). *Multi-hazard loss estimation methodology earthquake model*. Technical Manual. Department of Homeland Security Emergency Preparedness and Response Directorate FEMA Mitigation Division, Washington, D.C.

Hwang, H., Liu, J.B., and Chiu, Y-H. (2001). Seismic fragility analysis of highway bridges. *MAEC report: project MAEC RR-4*. Urbana: Mid-America Earthquake Center, 2001.

Mander, J.B., Kim, D.K., Chen, S.S., and Permus, G.J. (1996). Response of steel bridge bearings to the reverse cyclic loading. *Technical Report Technical Report NCEER-96-0014*, November 13, 1996.

Maragakis, E., Douglas, B., and Vrontinos, S. (1991). Classical Formulation of the Impact between Bridge Deck and Abutments during Strong Earthquakes. *Proceedings of the 6th Canadian Conference on Earthquake Engineering*, Toronto, Canada.

McKenna, F., Fenves, G.L., and Scott, M.H. (2004). OpenSees: Open System for Earthquake Engineering Simulation. *Pacific Earthquake Engineering Research Centre*, University of California, Berkeley, CA. http://opensees.berkeley.edu.

Menegotto, M., and Pinto, P.E. (1973). Method for analysis of cyclically loaded reinforced concrete plane frames including changes in geometry and non-elastic behavior of elements under combined normal force and bending. *Proceedings of IABSE Symposium on Resistance and Ultimate Deformability of Structures Acted on by Well-Defined Repeated Loads*, Lisbon, Portugal.

Muntasir Billaha, A.H.M., and Shahria Alamb, M. (2015). Seismic Fragility Assessment of Concrete Bridge Pier Reinforced with Superelastic Shape Memory Alloy. *Earthquake Spectra*, 31, 1515-1541.

Nielson, B.G., and DesRoches, R. (2007). Seismic fragility methodology for highway bridges using a component level approach. *Earthquake Engineering and Structural Dynamics*, 36, 823-839.

Ozbulut, O.E., Hurlebaus, S., and Desroches, R. (2011). Seismic response control using shape memory alloys: a review. *Journal of Intelligent Material System and Structures*, 22(14), 1531-1549.

Padgett, J.E., and DesRoches, R. (2007). Bridge functionality relationships for improved seismic risk assessment of transportation networks. *Earthquake Spectra*, 23(1), 115-130.

Padgett, J.E., DesRoches, R., and Ehlinger, R. (2010a) Experimental response modification of a four-span bridge retrofit with shape memory alloys. *Structural Control Health Monitoring*, 17(6), 694-708.

Padgett, J.E., Dennemann, K., and Ghosh, J. (2010b). Risk-based seismic life-cycle cost–benefit (LCC-B) analysis for bridge retrofit assessment. *Structural Safety*, *32*(3), 165-173.

PEER (Pacific Earthquake Engineering Research Center) (2013). *PEER Ground Motion Database*, University of California, Berkeley, CA (http://ngawest2.berkeley.edu/).

Scott, B.D., Park, P., and Priestley, M.J.N. (1982). Stress-strain behavior of concrete confined by overlapping hoops at low and high strain rates. *Journal of American Concrete Institute*, 79(1), 13-27.

Shinozuka, M., Feng, M.Q., Kim, H-K., and Kim, S-H. (2000). Nonlinear static procedure for fragility curve development. *Journal of Engineering Mechanics*, 126 (12), 1287-1295.

Song, G., Ma, N., and Li, H.N. (2006). Application of shape memory alloys in civil structures. *Engineering Structures*, 28, 1266-1274.

Song, J., and Kang, W.H. (2009). System reliability and sensitivity under statistical dependence by matrix-based system reliability method. *Structural Safety*, 31(2), 148-156.

Stein, S.M., Young, G.K., Trent, R.E., and Pearson, D.R. (1999). Prioritizing scour vulnerable bridges using risk. *Journal of Infrastructure Systems*, 5(3), 95-101.

Tremblay, R., Lacerte, M., and Christopoulos, C. (2008). Seismic Response of Multistory Buildings with Self-Centering Energy Dissipative Steel Braces. *Journal of Structural Engineering*, 134(1), 108-120.

USGS (2017). Unified hazard tool (https://earthquake.usgs.gov/hazards/interactive/).

Warn, G.P., and Whittaker, A.S. (2004). Performance estimates in seismically isolated bridge structures, *Engineering Structures*, 26(9), 1261-1278.

Wen, Y.-K., and Kang, Y. (2001). Minimum building life-cycle cost design criteria. I: Methodology. *J. Struct. Eng.*, 127, 3(330), 330–337.

Xue S., and Li X. (2007). Control devices incorporated with shape memory alloy. *Earth. Eng.*

Eng. Vib., 6(2),159–169.

Yi, J-H., Kim, S-H., and Kushiyama, S. (2007). PDF interpolation technique for seismic fragility analysis of bridges. *Eng Struct.*, 29, 1312-1322.

Zhang, J., and Huo, Y. (2009). Evaluating effectiveness and optimum design of isolation devices for highway bridges using the fragility function method. *Engineering Structures*, 31, 1648-1660.